Optimal layout of parallel power cables to minimize the stray magnetic field

(Article begins on next page)

05 January 2025

Optimal layout of parallel power cables to minimize the stray magnetic field

Luca Giaccone*

Politecnico di Torino, Dipartimento Energia,

corso Duca Degli Abruzzi, 24 - 10129 Torino

Abstract

This paper deals with three-phase power lines operated by parallel power cables. In these systems each phase is made up of several parallel subconductors and it is well known that the sequence of the subconductors influences the magnetic field generated by the power line. This paper proposes a new approach to identify the optimal arrangement of the power cables that minimizes the stray magnetic field. Unlike the design methods covered by the literature, this paper proposes a deterministic procedure that is based mainly on a simple geometrical indicator. This geometrical quantity makes it possible to analyze all the configurations in order to create a small subset of candidate solutions. From this subset the optimal solution is then identified quickly and easily by computing and comparing the stray field. A full validation of the proposed approach is performed by comparing it with a standard method based on genetic algorithm. The results of the validation also provide a useful table that covers all the cases from 2 to 6 subconductors for each phase. Furthermore, it is shown that the geometrical indicator makes it possible to obtain a good cable arrangement in a direct way, without performing any magnetic field evaluations.

keywords: magnetic field; stray field; parallel cables; optimization; current unbalance.

1   Introduction

Power delivery of electrical energy often requires cables with high ampacity. Two chief examples are industrial sector, where a large amount of power is required, and medium-voltage/low-voltage (MV/LV) substations where the conversion from medium to low voltage is accompanied by the increase of the current values on the LV side. Dealing with the necessity of the delivery of high current values, a possible solution is the adoption of busbar systems because of their

---

*Contact: `luca.giaccone@polito.it`

compactness and their ease of installation. The main drawback of this solution is the high frequency of the maintenance required to assure proper behavior of the system. An alternative solution is to use a power line made of parallel cables. Parallelism of more than one cable is unavoidable in order to reach the desired ampacity and, at the same time, to have the possibility to follow a desired path with flexible cables that can be folded easily. The literature has analyzed the systems made of parallel power cables because of the possible issues that can arise. First of all, the total current is not always shared equally by the subconductors belonging to the same phase [1, 2, 3], and this occurs for systems realized with busbars [4] or cables [5, 6]. The unbalance of the currents inside subconductors gives rise to other issues related to mechanical and thermal design. The electrodynamic stresses are not divided equally among the subconductors and those with higher currents heat up more than expected [3, 7]. Although it is possible for all these aspects to be taken into account by means of appropriate methodologies covered by the literature [8, 9, 10, 11], awareness and evaluation of the problem alone do not solve the issue itself. Therefore, a dedicated design methodology is necessary.

Another highly important issue nowadays is the emission of the magnetic field by electrical installations. Most countries have a regulatory framework on the exposure to electric and magnetic fields based on the ICNIRP guidelines [12] or on the IEEE standards [13]. For this reason the minimization of the magnetic field generated by parallel power cables has been already analyzed in the literature. Reference [14] shows the magnetic behavior of several power line layouts pointing out, for each case, the best and the worst cable arrangement. Reference [15] focuses on underground power cable duct banks. The paper identifies the best passive shield that minimizes the total cost (including the losses) depending on the cable configuration. The target of the optimization is very challenging ($B < 1$ μT), therefore, the authors highlight the importance of a proper management of the power cables to minimize as much as possible the magnetic field before the shield has to be designed and applied. Reference [5] is mainly related to the methodology for approaching the optimization problem. The authors want to test the performance of the optimization technique called Vector Immune System (VIS) [16] solving a multiobjective combinatorial problem. They seek the minimum magnetic field emission and the minimum unbalance of the currents. Even if power lines with parallel cables are simply used as a case study, some interesting conclusions are drawn in this reference. First of all, they find that the two objectives are slightly conflicting and therefore, the minimum magnetic field arrangement also becomes the most convenient one for the thermal and mechanical aspects.

In this paper we exploit the main conclusions of reference [5] in order to provide a simpler and effective method for the identification of the best arrangement of parallel power cables. The authors of [5] affirm that the optimal sequences are characterized by a geometrical symmetry. This concept is used to define a geometrical indicator based on the barycenter of the three phases. This indicator is used to analyze all possible permutations for a given number of subconductors. This analysis aims to select some candidate solutions in which

the best sequence is subsequently identified quickly and easily. In the rest of the paper this methodology will be described in detail and validated by comparing the results with a standard approach based on genetic algorithm (GA). Moreover, it will be shown that the simple geometrical interpretation of the problem provides interesting results without any dedicated optimization technique or special efforts.

2   Nomenclature

In this paper three-phase balanced power systems operated by parallel power cables are analyzed. A generic arrangement is uniquely described by the parameters summarized in Table 1.

TABLE 1: Parameters used to describe a power line arrangement.

N_T	total number of cables
N_S	number of subconductors composing each phase
N_R	number of rows
N_C	number of columns
Δ_x	distance between two consecutive cables along x direction
Δ_y	distance between two consecutive cables along y direction

It is worth noting that the parameters listed in Table 1 are not independent to each other. Indeed, the following relation alway holds: $N_\mathrm{T} = N_\mathrm{R} N_\mathrm{C} = 3 N_\mathrm{S}$. It is convenient to introduce all the parameters to provide clearer and more effective explanations of later notions.
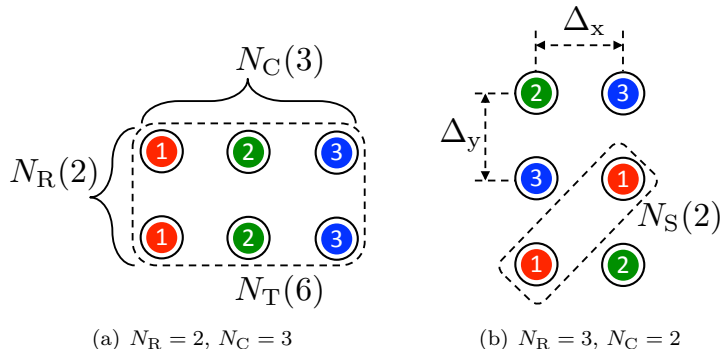

(a) $N_\mathrm{R} = 2$, $N_\mathrm{C} = 3$ (b) $N_\mathrm{R} = 3$, $N_\mathrm{C} = 2$

Figure 1: System of $N_\mathrm{T} = 6$ cables arranged in two configurations: ($N_\mathrm{R} = 2$, $N_\mathrm{C} = 3$) (a) and ($N_\mathrm{R} = 3$, $N_\mathrm{C} = 2$) (b).

After describing the arrangement of the power line, information about the position of the cables has to be provided. The three phases are identified with the numbers 1, 2 or 3. Moreover, they are also identified by a color that is red, green or blue, respectively. Bearing all this in mind, a cable sequence is described by N_T elements; each sequence includes N_S elements equal to 1, 2 and 3 (remember that $N_T = 3N_S$). With reference to Fig. 1 we analyze the example of a power line with $N_T = 6$ cables arranged in two configurations: $(N_R, N_C) = (2, 3)$ in Fig. 1(a) and $(N_R, N_C) = (3, 2)$ in Fig. 1(b). The sequence is filled reading the matrix of cables by rows. Starting from the bottom, we move from the lower left cable until the upper right. According to this rule, Fig. 1(a) and Fig. 1(b) both correspond to the sequence (123123). This example is given to highlight that the same sequence corresponds to significantly different cable positions depending of the arrangement defined by N_R and N_C. Finally, since the optimal sequence of the conductors is independent of the variables Δ_x and Δ_y, in this paper they are both fixed to the value of 5 cm.

3 General aspects

3.1 Objective function

In this paper, given an arrangement of cables, we identify a sequence that minimizes the generated magnetic field. Without loss of generality, all the magnetic field computations will be referred to the same inspection line as described in Fig. 2. The barycenter of the whole system corresponds with the origin of the system of coordinate. The 2 m long inspection line is centered with respect to the origin and it is 1 m far from the origin/cables.
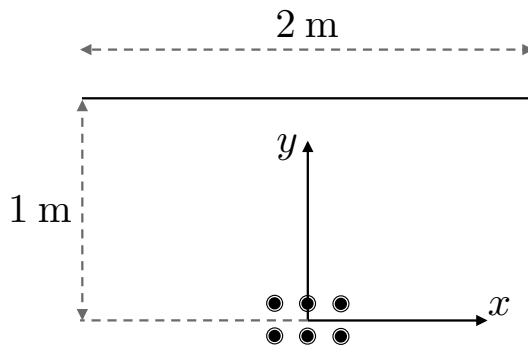

Figure 2: Description of the inspection line used to compute the magnetic flux density. The same inspection line is used throughout all the paper.

To identify the optimal sequence, the inspection line is discretized in Q points. The magnetic flux density is evaluated with the Ampére's law at each

point and the objective function (OF) is given by:

$$OF = \min\{\max\{B_j\}\} \ , \ j = 1\ldots Q \tag{1}$$

being B_j the rms value of the magnetic flux density at the jth point.

3.2 Problem assumptions

Assuming that the above introduced optimal sequence is found, in order to reorganize the system of conductors it is essential to know the original sequence. Even if this concept can be obvious, sometimes it is the main obstacle for the implementation of the optimal sequence. In fact, if the analysis is related to an already working circuit, the existing conductors sequence might be not known. In these cases it has to be identified by means of measurements. However, the identification is not always an easy task.

The proposed methodology is very suitable for the design of new cable arrangements. For parallel cables, it is well know that the mutual coupling between each other depends only on the geometry. This coupling can lead to a significant unbalance of the currents among subconductors. The problem is well investigated in the literature because of the above mentioned issues regarding thermal and mechanical aspects[3, 4, 17]. In this paper we assume that each cable carries the same share of the total phase current despite the possible mutual coupling. This assumption does not affect the final result as explained in the following.

Since we are looking for the sequence that minimizes the generated magnetic field, it is possible to neglect the unbalance for two reasons: 1) the literature points out that the minimization of the magnetic field and the minimization of the unbalance are two slightly conflicting objectives [5]. Hence, searching for one objective is like to search also for the other. 2) For a given sequence of conductors, the magnetic field related to a balanced current distribution does not differ significantly from the one obtained by the true current distribution.These two points guarantee that throughout whichever optimization procedure aimed to find the optimal sequence, the assumption of balanced currents does not compromise the process because a non-optimal sequence is discarded independently of the current distribution. Moreover, according to point 1, once the optimal solution is found the assumption of balanced currents correspond to the true physical distribution with a good approximation.

A numerical support is provided to the above considerations. Let us analyze 6 conductors with cross section equal to 240 mm^2. The conductors arrangement is identified by $(N_\mathrm{R}, N_\mathrm{C}) = (1, 6)$ and the distance between two conductors is one diameter. We analyze three cases: a) standard sequence (112233) imposing balanced currents in subconductors, b) standard sequence (112233) considering the true current distribution in subconductors, c) optimal sequence (123321) considering the true current distribution in subconductors. The last sequence is taken from [5] and confirmed later by the method under analysis. The true current distribution is evaluated taking into account skin and proximity effects

by means of a standard 2D finite element method [18]. The material considered is copper with conductivity $\sigma = 55$ MS/m. Table 2 summarizes the current values in the system. In the first case each subconductor carries 500 A whereas the second case presents the true current distribution for the same sequence. For the standard sequence (112233) the true current distribution correspond to an unbalanced system of subconductors. Finally, case "c" presents the true current distribution for the optimal sequence. It is important to observe that, the conductors sequence that minimizes the magnetic field makes also possible to have a balanced current distribution in subconductors. For the sake of completeness, Fig. 3 compares the magnetic flux density of the three cases along the inspection line. Firstly, it is confirmed the performance of the optimal sequence (123321). Furthermore, it is observed that, as explained earlier, even assuming balanced currents in subconductors (case "a" instead of case "b"), the optimization procedure will seek the optimal sequence correctly. Finally, as shown in Table 2, the optimal sequence is characterized by balanced currents in subconductors according to the assumption.

TABLE 2: Influence of the sequence on the magnitude of the current flowing in subconductors.

Conductor position	1st	2nd	3rd	4th	5th	6th
Case a: (112233)	500.00 A	500.00 A	500.00 A	500.00 A	500.00 A	500.00 A
Case b: (112233)	459.78 A	568.96 A	673.18 A	400.06 A	608.33 A	393.05 A
Case c: (123321)	499.91 A	499.85 A	500.04 A	499.96 A	500.15 A	500.09 A

4 Geometrical optimization approach

In this section we will show how it is possible to identify an optimal layout of parallel power cables by means of a simple geometrical indicator related to the barycenter of each phase. Considering a three-phase power system whose phases are made of N_S subconductors, the total number of configurations is computed using the formula for the permutations of N_T elements with N_S items equal to 1 or 2 or 3:

$$P = \frac{N_\mathrm{T}!}{N_\mathrm{S}!N_\mathrm{S}!N_\mathrm{S}!} = \frac{N_\mathrm{T}!}{\left(N_\mathrm{S}!\right)^3} \tag{2}$$
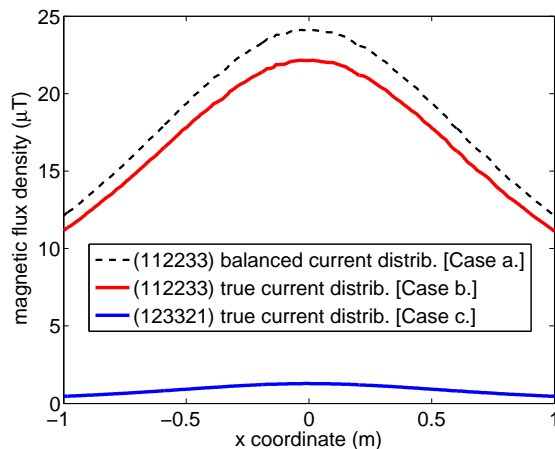
Figure 3: Magnetic flux density along the inspection line for: standard sequence (112233) imposing balanced currents, standard sequence (112233) with true current distribution, optimal configuration (123321) with true current distribution.

For a given configuration one can compute the barycenter of each phase as

$$\vec{G}_k = \frac{1}{N_{\mathrm{S}}} \sum_{j=1}^{N_{\mathrm{S}}} \vec{r}_{k,j} \ , \quad \mathrm{k} = 1, 2, 3 \tag{3}$$

being $\vec{r}_{k,j}$ the position of the jth subconductor belonging to the kth phase. Now the three barycenter-to-barycenter distances can be computed as:

$$\vec{D}_{ij} = \vec{G}_i - \vec{G}_j \ , \quad \forall \ i \neq j \tag{4}$$

An example of these quantities is given in Fig. 4 where the configuration $(N_{\mathrm{R}}, N_{\mathrm{C}}) = (3, 4)$ and the conductors sequence (122212131333) are considered.

Finally, the following geometrical indicator is defined

$$d = D_{12} + D_{23} + D_{31} \tag{5}$$

being $D_{ij} = \left| \vec{D}_{ij} \right|$.

The geometrical optimization is based on the quantity d. Its value is computed for all the possible permutations of the given arrangement. Afterwards, it is used to dramatically reduce the number of candidate solutions. The procedure selects all the configurations with the minimum value of d and defines them as a subset of candidate permutations (hereinafter defined with the symbol P_{S}) between which the best sequence has to be found. To provide an idea of how the selection based on the d values behaves, we have to look at Table 3. It is quite clear that, by increasing the number of subconductors N_{S}, the computation of
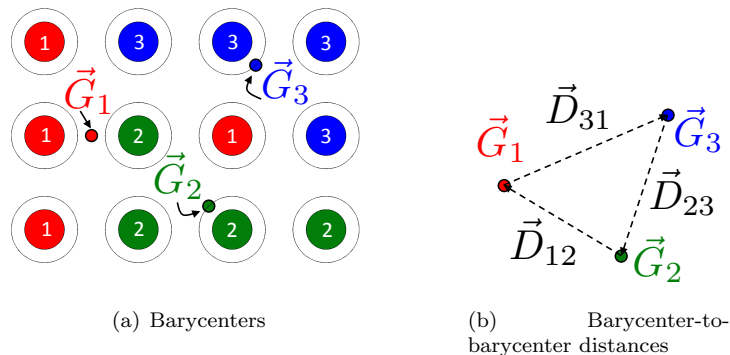
Figure 4: Representation of the barycenters (a) and the barycenter-to-barycenter distances (b) for the configuration $(N_\mathrm{R}, N_\mathrm{C}) = (3, 4)$ and conductors sequence (122212131333).

the magnetic field for all the permutations P becomes quickly impractical. On the other hand, the subset of candidate solutions P_S includes few components of the complete set P. Table 3 points out that the value of P_S is dependent on the arrangement $(N_\mathrm{R}, N_\mathrm{C})$. Moreover, column 4 provides the percentage of the candidate solutions with respect to the total permutations. It is interesting to see that this value is always lower than 1 % for $N_\mathrm{S} > 2$. Therefore, the geometrical selection makes it possible to analyze all the candidate solutions P_S with reasonable efforts and computational times (in the order of few seconds as it will be detailed later). Regarding the implementation of the geometrical selection a further important remark has to be given. The identification of the candidate solutions is performed on the whole set of permutations P. The computation can be performed very fast even for a huge number of configurations if the environment employed allows for vectorial analysis (e.g. MATLAB, Python). Once the value of d is known for all the permutations one has to look for the permutations characterized by the lowest value of d. Without loss of generality, let us consider the case in which the lowest possible value is exactly zero (as often happens). From the numerical viewpoint, it is mandatory to look for the lowest possible value of d with a given tolerance to avoid the unwanted discard of the best solution due to numerical inaccuracy (e.g. $d = 10^{-19}$ m instead of $d = 0$ m).

Another remark has to be given regarding the main limitation of the method. As already said, the geometrical indicator d is evaluated for all the possible permutations. As shown in Table 3 the number of permutations grows dramatically as the number of subconductors increases. The amount of permutations to be analyzed simultaneously puts a "physical" limitation to the number of subconductors that can be analyzed on a given machine. In this paper all the simulations are carried out on a laptop with the following hardware: Intel Core i7 dual-core, 2.8 GHz, 16 GB of RAM. Consequently, the maximum value of N_S

8

TABLE 3: Geometrical selection behavior

N_S	(N_R, N_C)	P	P_S	P_S/P (%)
2	(1,6)	90	6	6.67
	(2,3)		6	6.67
3	(1,9)	1 680	12	0.71
	(3,3)		12	0.71
4	(1,12)	34 650	192	0.55
	(2,6)		168	0.48
	(3,4)		150	0.43
5	(1,15)	756 756	1830	0.24
	(3,5)		1 134	0.15
6	(1,18)	17 153 136	25986	0.15
	(2,9)		16 224	0.09
	(3,6)		14 076	0.08

that can be analyzed is 6 because the associated permutations requires only 2.4 GB of RAM. The analysis of systems with $N_S = 7$ becomes unfeasible on this machine because the required RAM for allocating the matrix P is approximately 70 GB.

Finally, it must be stressed that among all the candidate solutions P_S, more than one optimal solution can be found because some sequences are completely equivalent even if apparently different. Equivalent sequences can be obtained, for example, applying a circular rotation of phases ($123 \rightarrow 312 \rightarrow 231$) or by mirroring an optimal sequence [5]. In this paper we will present only one optimal sequence because the other equivalent sequences can be defined according to the procedures cited above.

5 Validation

The purpose of this section is the validation of the proposed approach based on geometrical concepts. For that reason, we make use of a standard technique based on a genetic algorithm [19, 20]. The optimization under analysis has a lot of similarities with the Traveling Salesman Problem (TSP) which is a classical combinatorial problem. The TSP problem is very well analyzed in [21]. Following the suggestion of this reference, in this paper each candidate solution is described by means of the *path encoding* that is considered to be the most natural one for combinatorial problems. Moreover, according to reference [22] in the GA process new generations are created by means of the *partially mapped crossover* (PMX) and the *simple inversion mutation* (SIM). These genetic op-

erators are presented in [21] but, actually, due to the peculiarity of the problem under analysis (repeated elements), the SIM operator is slightly modified to assure that, once the mutation is performed, the resulting chromosome is different from the starting one [5].

All the possible configurations varying N_S from 2 to 6 are analyzed. The GA and the proposed approach are used to identify the best sequences. For all the configurations the two methods provide the same optimal sequence. The results are summarized in Table 4 with other additional information regarding the computational time that will be commented in the following. The proposed

TABLE 4: Best sequences and computational times

N_S	(N_R, N_C)	Optimal sequence	$10 \times t_{GA}$ (s)	t_{geom} (s)
2	(1,6)	(123321)	18.2	0.001
	(2,3)	(123321)		0.003
3	(1,9)	(123312231)	19.6	0.005
	(3,3)	(123231312)		0.004
4	(1,12)	(123321321123)		0.05
	(2,6)	(123231321132)	21.6	0.04
	(3,4)	(122333112132)		0.04
5	(1,15)	(123233111223231)	48.0	0.80
	(3,5)	(122313331221123)		0.72
6	(1,18)	(123321321123123321)		26.00
	(2,9)	(123231312321132213)	1 454.3	22.93
	(3,6)	(122331331122213213)		21.56

approach is a deterministic method and hence, it is simple to quantify the computational time because it mainly depends on the value of P_S. The values are listed in the last column of Table 4. Regarding the genetic algorithm, it must be remembered that it belongs to the family of heuristic optimization techniques. Therefore, it is not assured to reach the global optimum with one single run. In this paper the GA is used 10 times for each configuration and the best solution among the 10 results is considered to be the global optimum. This is the reason why in column 4 the computational time of the GA is provided as "$10 \times t_{GA}$", where t_{GA} is the elapsed time of a single run. The value of t_{GA} is mainly influenced by the parameters of the GA as: *population size* and *maximum number of allowed generations*. These parameters are kept constant for a given value of N_S, hence, only one value is given for different arrangements. For N_S up to 5 the population size and the maximum allowed generations are set to 200 and 100, respectively. For $N_S = 6$, unlike the previous cases, these

10

parameters have to be increased to 1000 and 1500, respectively, to ensure the identification of the global optimum within the above mentioned 10 runs. This requirement justifies the significant increase of the computational time of the GA for the three arrangements with 6 subconductors.

Bearing all this in mind, Table 4 puts in evidence that the geometrical optimization reaches the same results of the GA requiring a lower computational time.

6   Direct application

In this paper a geometrical concept is used to define a deterministic procedure that, as described previously, provides the optimal sequence of a set of parallel cables. In this section we want to emphasize that the geometrical indicator (5) is a self sufficient concept which ensures satisfactory results. First of all, we provide some reference performance considering the configurations of Table 4 in which the cables are arranged by rows. We compute the *shielding factor* (SF) defined as the ratio between the field before the mitigation and the mitigated field. The most common way to arrange the conductors is to install all the subconductors belonging to a single phase close to each other. This kind of sequence is taken as reference case. Hence, the magnetic field related to this kind of configuration is considered as the unmitigated field in the computation of the shielding factor. To give a concrete example, for a system with $N_S = 3$ that is arranged by rows, $(N_R, N_C) = (3, 3)$, the standard sequence is (111222333).

The SF, by definition, is a pointwise function of the space, here we compute the SF along the same inspection line used in the optimizations. The results presented in Fig. 5 show that very high values of SF can be obtained when the number of subconductors N_S increases.
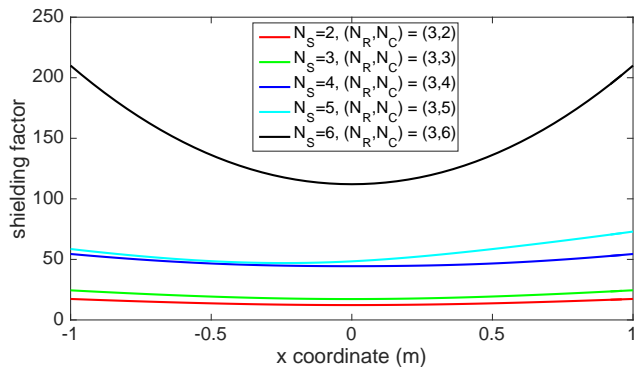

Figure 5: Shielding factors along the inspection line for the configurations in which the cables are arranged by rows. These values are provided to give some reference performance for a later comparison.

As already pointed out, this section demonstrates that simply using the geometrical indicator defined in (5) it is possible to obtain satisfactory results. Let us consider a three phase system with $N_S = 8$ subconductors for each phase. The subconductors are arranged by rows as $(N_R, N_C) = (3, 8)$. For this system the best sequence is not available in Table 4, however, it is possible to observe that the minimization of the geometrical indicator d occurs when the cables are positioned with a good degree of symmetry. This concept enables everyone to classify a cable sequence with reference to the magnetic field emission without the computation of the magnetic field. Here, we test the trial sequence described in Fig. 6 in the right inset. The sequence is defined manually a priori and, to complete the comparison, the magnetic flux density along the inspection line is computed in order to define the SF (referred to the relative standard configuration represented in Fig. 6). In the end, it is possible to observe that, even without an optimization, the geometrical concept makes it possible to reach really good results. The average SF along the inspection line is approximately 50, a high value that is often sufficient to solve any issues created by the dispersed magnetic field. This approach have been profitably used by the author of this paper and his colleagues for the optimization of a low voltage power line related to very complex substations [23].
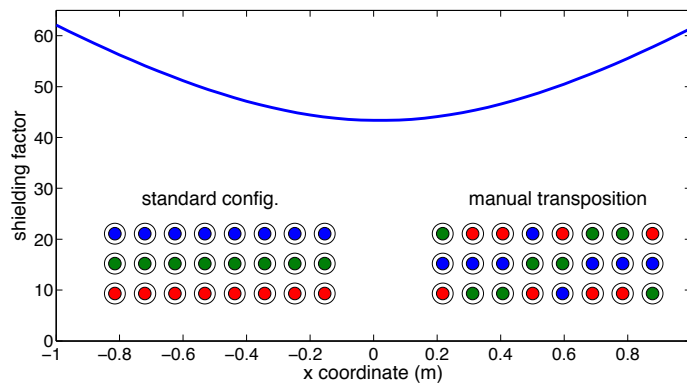

Figure 6: Shielding factors along the inspection line obtained by manually defining a symmetric sequence for a system with $N_S = 8$ subconductors for each phase.

7   Conclusions

In this paper a new methodology to identify the optimal sequence of a power line made of parallel cables is proposed. According to the literature, for the magnetic field emission and the balance of the current among the subconductors of the same phases, the optimal cable arrangement is characterized by a good symmetry of the cable positions. The proposed methodology exploits this concept

by computing the barycenter of each phase and further defining a geometrical indicator (d) obtained as the average of the barycenter-to-barycenter distances. The value of d is used to select some candidate solutions among all the possible permutations. The best sequence is then identified quickly and easily because the geometrical selection dramatically reduces the amount of possible solutions.

The proposed method was validated by comparing its results with those obtained by means of a standard approach based on genetic algorithm. All the cable arrangements with a number of subconductors up to 6 were analyzed. First of all, a perfect agreement was found between the proposed approach and the GA. Moreover, the proposed approach provided performance improvements with reference to the computational time.

Finally, a system with 8 subconductors for each phase was used to emphasize that the rationale of the method is a powerful concept because, due to its simplicity, very good results can be obtained even without a formal optimization procedure. It is sufficient to identify an arrangement characterized by a good symmetry of the cable positions. In other words, the rationale of the geometrical approach makes it possible to reach interesting results without performing a real magnetic field analysis of the system.

References

[1] F. P. Dawson, M. Cao, P. K. Jain, A simplified approach to calculating current distribution in parallel power buses, IEEE Trans. Magn. 26 (2) (1990) 971–974.

[2] K. A. Petty, Calculation of current division in parallel single-conductor power cable for generating station applications, IEEE Trans. Power Del. 6 (2) (1991) 479–487.

[3] K. Gouramanis, C. Demoulias, D. P. Labridis, P. Dokopoulos, Distribution of non-sinusoidal currents in parallel conductors used in three-phase four-wire networks, Electr. Power Syst. Res. 79 (2009) 766–780.

[4] M. Chiampi, D. Chiarabaglio, M. Tartaglia, A general approach for analyzing power busbar under ac conditions, IEEE Trans. Magn. 29 (6) (1993) 2473–2475. doi:10.1109/20.280979.

[5] A. Canova, F. Freschi, M. Tartaglia, Multiobjective optimization of parallel cable layout, IEEE Trans. Magn. 43 (10) (2007) 3914–3920.

[6] F. Freschi, M. Tartaglia, Power lines made of many parallel single-core cables: A case study, IEEE Trans. Ind. Appl. 49 (4) (2013) 1744–1750.

[7] P. Y. Du, X. H. Wang, Electrical and thermal analyses of parallel single-conductor cable installations, IEEE Trans. Ind. Appl. 46 (4) (2010) 1534–1540.

[8] N. Kovac, I. Sarajcev, D. Poliak, Nonlinear-coupled electric-thermal modeling of underground cable systems, IEEE Trans. Power Del. Vol. 21 (2006) 4–14.

[9] D. P. Labridis, D. P. Labridis, P. S. Dokopoulos, Electromagnetic forces in three-phase rigid busbars with rectangular cross-sections, IEEE Trans. Power Del. 11 (2) (1996) 793–800. doi:10.1109/61.489336.

[10] A. Canova, L. Giaccone, Numerical and analytical modeling of busbar system, IEEE Trans. Power Del. 24 (3).

[11] B. Novák, L. Koller, Current distribution and losses of grouped underground cables, IEEE Trans. Power Del. 26 (3) (2011) 1514–1521.

[12] ICNIRP, Guidelines for Limiting Exposure to Time-Varying Electric and Magnetic Fields (1 Hz - 100 kHz), Health Phys 99 (6) (2010) 818–836.

[13] C95.6 - IEEE standard for safety levels with respect to human exposure to electromagnetic fields, 0 - 3 kHz.

[14] M. M. Dawoud, I. O. Habiballah, A. S. Farag, A. Firoz, Magnetic field management techniques in transmission underground cables, Electr. Power Syst. Res. 48 (1999) 177–192.

[15] J. C. del Pino-López, P. Cruz-Romero, L. Serrano-Iribarnegaray, Martínez-Román, Magnetic field shielding optimization in underground power cable duct banks, Electr. Power Syst. Res. 114 (2014) 21–27.

[16] F. Freschi, M. Repetto, Vis: An artificial immune network for multi-objective optimization, Eng. Optim 38 (8) (2006) 975–996.

[17] O. Bottauscio, E. Carpaneto, M. Chiampi, D. Chiarabaglio, I. Panaitescu, Numerical and experimental evaluation of magnetic field generated by power busbar systems, IEE Proc.-gener. transm. distrib. 143 (5) (1996) 455–460.

[18] D. C. Meeker, Finite Element Method Magnetics, available: http://www.femm.info/, version 4.2 (Dec. 2006).

[19] J. H. Holland, Adaptation in Natural and Artificial Systems, Ann Arbor, MI: The Univ. of Michigan Press, 1975.

[20] D. E. Goldberg, Genetic Algorithms in Search, Optimization, and Machine Learning, Addison-Wesley, 1989.

[21] P. Larrañga, C. M. H. Kuijpers, R. H. Murga, I. Inca, S. Dizdarevic, Genetic algorithms for the travelling salesman problem: A review of representations and operators, Artif. Intell. Rev. 13 (2) (1999) 129–170.

[22] P. Larrañga, C. M. H. Kuijpers, R. H. Murga, Y. Yurramendi, Learning bayesian network structures by searching for the best ordering with genetic algorithms, IEEE Trans. Syst., Man, Cybern. A, Syst.,Humans. 26 (4) (1996) 1996.

[23] D. Bavastro, A. Canova, F. Freschi, L. Giaccone, M. Manca, Magnetic field mitigation at power frequency: design principles and case studies, IEEE Trans. Ind. Appl. 51 (3) (2014) 2009–2016. doi:10.1109/TIA.2014.2369813.